# How to count kinks: From the continuum to the lattice and back

Marcelo Gleiser and Hans-Reinhard Müller

*Department of Physics and Astronomy, Dartmouth College, Hanover, NH 03755, USA*

(DART-HEP-97/07  February 1, 2008)

We investigate the matching between (1+1)-dimensional nonlinear field theories coupled to an external stochastic environment and their lattice simulations. In particular, we focus on how to obtain numerical results which are lattice-spacing independent, and on how to extract the correct effective potential which emerges from the simulations. As an application, we study the thermal production of kink-antikink pairs, obtaining a number density of pairs which is lattice-spacing independent and the effective barrier for pair production, *i.e.*, the effective kink mass.

The possibility that the Universe underwent a series of symmetry breaking phase transitions during the earliest stages of its evolution has triggered a great deal of interest in the application of nonequilibrium statistical mechanics to cosmology. Of particular interest is the potential role that coherent field configurations, which arise from the interplay between nonlinearities and out-of-equilibrium conditions, could have played in shaping the earlier evolution and present-day structure of the Universe. Examples range from the nucleation of bubbles in the context of inflation and electroweak baryogenesis to the formation of topological defects [1].

Given the relevance of the topic, and the obvious difficulties in performing experiments in a cosmological context, attempts to investigate the emergence of coherent field structures rely heavily on numerical simulations and possible analogies with condensed matter experiments [2]. Here we would like to focus on the former, namely, on numerical simulations designed to investigate the emergence of coherent structures in thermal field theories. An obvious limitation of such an approach is that, although field theories are continuous and usually formulated in an infinite volume, lattice simulations are discrete and finite, imposing both a maximum ("size of the box" $L$) and a minimum (lattice spacing $\delta x$) wavelength that can be probed by the simulation. When the system is coupled to an external thermal (or quantum) bath, fluctuations will be constrained within the allowed window of wavelengths, leading to discrepancies between the continuum formulation of the theory and its lattice simulations; the results will be dependent on the choice of lattice spacing.

Parisi suggested that if proper counterterms were used, this depedence on lattice spacing could be attenuated [3]. This technique was implemented in a study of 2-dimensional nucleation by Alford and Gleiser [4]. However, these studies still left open the question of how to match the lattice results to the correct continuum field theory. This is a crucial step if we want to test numerically certain predictions from field theories of relevance not only for cosmology but also for condensed matter physics, such as decay rates of metastable states and the production of topological defects. Recently, Borrill and Gleiser (BG) have examined this question within the context of 2-dimensional critical phenomena [5]. They have computed the counterterms needed to render the simulations indepedent of lattice spacing and have obtained a match between the simulations and the continuum field theory, valid within the one-loop approximation used in their approach. Inspired by their results, we decided to investigate the validity of this method within the context of topological defects. The results presented here should be relevant to numerical studies of the formation of topological defects and their comparison with experiments [6], as well as to elucidating the general nature of the effective potential which emerges from coupling nonlinear field theories to a stochastic thermal (or quantum) background.

## I. THE METHOD

The Hamiltonian for a classical scalar field with potential $V_0(\phi)$ and an environmental temperature $T$ is, (with $k_B = c = 1$)

$$\frac{H[\phi]}{T} = \frac{1}{T} \int dx \left[ \frac{1}{2} \left( \frac{\partial \phi}{\partial t} \right)^2 + \frac{1}{2} \left( \frac{\partial \phi}{\partial x} \right)^2 + V_0(\phi) \right] . \tag{1}$$

Even though 1-dimensional field theories are free of ultra-violet divergences, the ultra-violet cutoff imposed by the lattice spacing will generate a *finite* contribution to the effective potential which must be taken into account if we are to obtain a proper match between the theory formulated in Eq. (1) and its numerical simulation on a discrete lattice. If neglected, this contribution will compromise the measurement of physical quantities such as the density of kink-antikink pairs or the effective kink mass. However, before investigating the particular example of kink-antikink production, we present the method in its most general form.

For classical, 1-dimensional finite-temperature field theories, the one-loop corrected effective potential is given by the momentum integral [3]

$$V_{1L}(\phi) = V_0(\phi) + \frac{T}{2} \int_0^\infty \frac{dk}{2\pi} \ln\left[1 + \frac{V_0''(\phi)}{k^2}\right] = V_0(\phi) + \frac{T}{4}\sqrt{V_0''(\phi)} \,. \tag{2}$$

As mentioned before, the lattice spacing $\delta x$ and the lattice size $L$ introduce long and short momentum cutoffs $\Lambda = \pi/\delta x$ and $k_{\min} = 2\pi/L$, respectively. Lattice simulations are characterized by one dimensionless parameter, the number of degrees of freedom $N = L/\delta x$. For sufficiently large $L$ one can neglect the effect of $k_{\min}$ and integrate from 0 to $\Lambda$. For $V_0'' \ll \Lambda^2$ (satisfied for sufficiently large $\Lambda$), the result can be expanded into

$$V_{1L}(\phi, \Lambda) = V_0 + \frac{T}{4}\sqrt{V_0''} - \frac{T}{4\pi}\frac{V_0''}{\Lambda} + \Lambda T \, \mathcal{O}\left(\frac{V_0''^2}{\Lambda^4}\right) \,. \tag{3}$$

As is to be expected for a 1-dimensional system, the limit $\Lambda \to \infty$ exists and is well-behaved; there is no need for renormalization of ultra-violet divergences. However, the effective one-loop potential is lattice-spacing dependent through the explicit appearance of $\Lambda$, and so are the corresponding numerical simulations. In order to remove this dependence on $\delta x$, we follow the renormalization procedure given by BG [5]; it is irrelevant if the $\Lambda$-dependent terms are ultra-violet finite ($d = 1$) or infinite ($d \geq 2$). In the lattice formulation of the theory, we add a (finite) counterterm to the tree-level potential $V_0$ to remove the lattice-spacing dependence of the results,

$$V_{ct}(\phi) = \frac{T}{4\pi}\frac{V_0''(\phi)}{\Lambda} \,. \tag{4}$$

There is an additional, $\Lambda$-independent, counterterm which was set to zero by an appropriate choice of renormalization scale. The lattice simulation then uses the corrected potential

$$V_{latt}(\phi) = V_0(\phi) + \frac{T\delta x}{4\pi^2}V_0''(\phi) \,. \tag{5}$$

As we will show later in the context of kink-antikink pair production, this lattice formulation simulates the continuum limit to one loop as given by Eq. (2).

Note that the above treatment yields two novel results. First, that the use of $V_{latt}$ instead of $V_0$ gets rid of the dependence of simulations on lattice spacing. [Of course, as $\delta x \to 0$, $V_{latt} \to V_0$. However, this limit is often not computationally efficient.] Previous works [7], have explored the influence of a counterterm quadratic on lattice spacing. However, we note that for small enough $\delta x$, the limit of interest here, our linear correction is dominant. Second, that the effective interactions that are simulated must be compared to the one-loop corrected potential $V_{1L}(\phi)$ of Eq. (2); once the lattice formulation is made independent of lattice spacing by the addition of the proper counterterm(s), it simulates, within its domain of validity, the thermally corrected one-loop effective potential.

## II. APPLICATION: THERMAL NUCLEATION OF KINK-ANTIKINK PAIRS

As an application of the method discussed above we consider the symmetric double-well potential $V_0(\phi) = \frac{\lambda}{4}\left(\phi^2 - \phi_0^2\right)^2$. The excitations of the associated quantum theory have a mass $m = \hbar\omega = \hbar\sqrt{2\lambda}\,\phi_0$. Thus, in order for the system to remain in the classical regime, the condition $T \gg \hbar\sqrt{2\lambda}\,\phi_0$ must hold. This constrains the dimensionless temperature $\Theta = T/(\sqrt{\lambda}\phi_0^3)$ to be larger than $\sqrt{2}\hbar/\phi_0^2$. For $\Theta \ll \tilde{M}_k \equiv \sqrt{8/9}$, where $\tilde{M}_k$ is the dimensionless kink mass corresponding to the tree-level potential $V_0$ [8], we can expect to have only a dilute gas of kink-antikinks at thermal equilibrium. With these two conditions jointly satisfied, the system will also obey $M_K \equiv \sqrt{\lambda}\phi_0^3\tilde{M}_k \gg m$, indicating weak coupling.

The corrected lattice potential is

$$V_{\text{latt}}(\phi) = V_0(\phi) + \frac{3}{4\pi^2}\lambda T \delta x \phi^2 \; ; \tag{6}$$

simulations using $V_{\text{latt}}$ will, in principle, match the continuum theory

$$V_{\text{1L}}(\phi) = V_0(\phi) + \frac{T\sqrt{\lambda}}{4}\sqrt{3\phi^2 - \phi_0^2} \;, \tag{7}$$

which has (shifted) minima at $\pm\phi_{\min}(T)$, with $\phi_{\min}(T) < \phi_0$.

For the numerical simulations we introduce the dimensionless variables $\tilde{t} = \sqrt{\lambda}\phi_0\,t$, $\tilde{x} = \sqrt{\lambda}\phi_0\,x$, and $\tilde{\phi} = \phi/\phi_0$. To keep the notation simple we will subsequently suppress the tilde. The field is prepared as $\phi(t = 0) = -1$, and evolved in time according to a Langevin equation with white noise that incorporates the environmental temperature $T$ through the fluctuation-dissipation theorem. The details of this and of the numerical implementation are laid out in [5]. The viscosity coefficient $\eta$ has been set to unity throughout this study. The time step is $\delta t = 0.05$, and $L = 2100$. The heat bath takes a time $\Delta t \approx 3$ to achieve equipartition so that the energy per degree of freedom is $E/N = T/2$.

### III. RESULTS

**Ensemble average of field.** For sufficiently low temperatures the simulated field will remain in the vicinity of the minimum $\phi = -\phi_{\min}(T)$ for a very long time (compared to typical fluctuation time-scales), until large-amplitude fluctuations drive portions of the space over the barrier at $\phi = 0$ and beyond. The subsequent evolution is then the formation of the first kink-antikink pair. True thermal equilibrium consists of reaching the final equilibrium kink-antikink density together with zero mean field. In a lose sense, this situation corresponds to symmetry restoration, although in one spatial dimension "symmetry restoration" will occur for any nonzero temperature; it is all a matter of time.

As a first test of our procedure, we investigate the mean field value $\bar{\phi}(t) = (1/L)\int \phi(x,t)dx$ *before* the nucleation of a kink-antikink pair, *i.e.*, while the field is still well localized in the bottom of the well. In Fig. 1 we show the ensemble average of $\bar{\phi}$ (after 100 experiments) for different values of $\delta x$, ranging from 1 down to 0.1, at $T = 0.1$. The simulations leading to the left graphs use the "bare" potential $V_0$, whereas the right graphs are produced employing $V_{\text{latt}}$ (Eq. 6). Apart from a discrepancy for very coarse grids ($\delta x = 1$), where the resolution nears the correlation length, the average field value is clearly lattice-spacing independent when using $V_{\text{latt}}$, in contrast to the use of $V_0$.

As discussed before, the average mean field value should correspond to the minimum $-\phi_{\min}(T)$ of the effective potential. However, since we are only using a one-loop approximation, this agreement will get progressively worse as the temperature increases. For example, for $T = 0.2$, the discrepancy between the theoretical value, $-\phi_{\min}(0.2)$, and the numerical result is 10%. For higher temperatures, we should not trust the one-loop approximation; other nonperturbative effects, such as subcritical fluctuations, too small in width and amplitude to emerge as a kink-antikink pair but still large enough to bring the average value of the field away from its one-loop value, will become important [9]. Thus, we restrict our investigation to temperatures safely within the limits of validity of the one-loop approximation. In a subsequent study, we intend to investigate the role of these nonperturbative effects.

**Density of kink-antikink pairs.** Perhaps the most difficult task when counting the number of kink-antikink pairs that emerge during a simulation is the identification of what precisely is a kink-antikink pair at different temperatures. Typically, we can identify three "types" of fluctuations: i) small amplitude, perturbative fluctuations about one of the two minima of the potential; ii) full-blown kink-antikink pairs interpolating between the two minima of the potential; iii) nonperturbative fluctuations which have large amplitude but not quite large enough to satisfy the boundary conditions required for a kink-antikink pair. These latter fluctuations are usually dealt with by a smearing of the field over a certain length scale. Basically, one chooses a given smearing length $\Delta L$ which will be large enough to "iron out" these "undesirable" fluctuations but not too large that actual kink-antikink pairs are also ironed-out. In this study, a similar smoothing was implemented as a four-pole Butterworth low-pass filter of the field with a filter cutoff length $\Delta L$. The filter removes fluctuations with wavelengths smaller than $\Delta L$. The choice of $\Delta L$ is, in a sense, more an art than a science, given our ignorance of how to handle these nonperturbative fluctuations.

In Table 1 we show the number of pairs for different choices of filter cutoff length and for different temperatures. We counted pairs by identifying the zeros of the filtered field. From Table 1 it is clear that as the temperature increases, the discrepancies in the count of pairs also increase. For this reason we only trust our data for fairly low temperatures. The problem is agravated by the fact that the "size" of the kink-antikink pair, *i.e.*, the minimal separation between the two, not only changes due to dynamical effects, but also changes with temperature. Thus, choosing the filter cutoff length to be too large may actually undercount the number of pairs. Choosing it too low may include nonpertubative

fluctuations as pairs. We chose $\Delta L = 3$ in the present work, as this is the smallest "size" for a kink-antikink pair. In contrast, in the works by Alexander et al. a different method was adopted, that looked for zero-crossings for eight lattice units (they used $\delta x = 0.5$) to the left and right of a zero crossing [10]. We have checked that our simulations reproduce the results of Alexander et al. if we: i) use the bare potential in the lattice simulations and ii) use a large filter cutoo length $\Delta L$. Specifically, the number of pairs found with the bare potential for $T = 0.2$, $\delta x = 0.5$ are: $n_p = 36$, 30, and 27, for $\Delta L = 3$, 5, and 7, respectively. Alexander et al. found (for our lattice length) $n_p = 25$. Comparing these with Table 1, it is clear that the differences between our results and those of Alexander et al. come from using a different potential in the simulations, *viz.* a corrected vs. an uncorrected potential.

We believe that at this point it is fair to say that the "smearing issue" remains unresolved, at least for temperatures $T > 0.25$ or so. We intend to address the issue of how to deal with these nonperturbative effects in a forthcoming publication. In any case, the focus of the present work is mostly on how to achieve a lattice-independent count, irrespective of the particular method used for identifying the kink-antikink pairs.

Fig. 2 compares measurements of the kink-antikink pair density (half the number of zeros of the filtered field), ensemble-averaged over 100 experiments, for different lattice spacings. Again it is clear from the graphs on the left that using the tree-level potential $V_0$ in the simulations causes the results to be dependent on $\delta x$, whereas the addition of the finite counterterm removes this problem quite efficiently; both diagrams of Fig. 2 contain four graphs each, although the graphs on the right are almost indistinguishable. Unless the properly corrected potential is used in the lattice simulations, the measured number density of topological defects is sensitive to the lattice spacing. One must be careful when counting kinks, especially for large lattice spacings, say $\delta x = 0.25$ or larger.

The next step is to extract the correct continuum theory from the lattice simulations. What theory is the lattice simulating? Most previous simulations of thermal nucleation of kink-antikink pairs have overlooked this problem. Although a temperature-dependent kink mass was conjectured in the works of reference [11], not much has been done to understand its origin or its value. One way of addressing it is by comparing the numerically measured kink mass with its theoretical prediction. It has been found that the measured mass was smaller than the theoretical prediction by a factor ranging from 25% to 45% [11,12], a disturbing result. This has been attributed to several effects, such as the finite size of the lattice, the finite size of the kinks, and phonon dressing effects due to the lattice discretization [13]. We will show that this problem is rooted in the incorrect matching between theory and numerical simulations. In the works by Alexander et al. a beautiful agreement between the low temperature limit and a $T = 0$ WKB approximation was obtained, as well as between high temperatures and a double Gaussian nonperturbative method [10]. Our method is effective precisely between these two regimes, and could be interpreted as a $T$-dependent WKB approximation obtained naturally from the inclusion of counterterms.

One should expect the equilibrium kink-antikink pair density to follow the proportionality [14]

$$n_{\text{kink}} \propto \frac{1}{\sqrt{T}} \exp(-M_k/T) \tag{8}$$

where $M_k$ is the kink mass, given by

$$M_k = \int dx \left[ \frac{1}{2}\phi_k'^2 + V(\phi_k) \right] , \tag{9}$$

and $\phi_k(x)$ is the kink solution to the equation of motion. Note that we left the potential $V(\phi_k)$ unspecified. If we use the tree-level potential, $V_0(\phi_k)$, we obtain the well-known result $M_k = \sqrt{8\lambda/9}\phi_0^3$. Or, in dimensionless variables, $\tilde{M}_k = \sqrt{8/9}$. One can extract the numerical value of $M_k$ by measuring the pair density and plotting the results in a logarithmic scale, as in Ref. [12]. The result should be a straight line with negative slope $-\tilde{M}_k = -\sqrt{8/9}$. However, as mentioned above, the measured slope was found to be about $-0.70\tilde{M}_k$. The reason for the discrepancy is that the potential which should be used when comparing theory and simulation is not the tree-level potential $V_0(\phi)$ but the effective potential $V_{1L}(\phi)$. Thus, one must compute the effective kink mass $M_k(T)$ using the corrected potential $V_{1L}(\phi)$ and *then* compare the results with the numerical simulations.

The effective kink mass can be found using the equation of motion and the real part of $V_{1L}$ [15],

$$M_k(T) = \int dx \left[ \frac{1}{2}\phi_k'^2 + \text{Re}(V_{1L}) \right] = 2\int_0^{\phi_{\min}} \sqrt{2\text{Re}(V_{1L}(\phi))} \, d\phi . \tag{10}$$

This integration can easily be carried out numerically. In Fig. 3 we plot the ratio $\tilde{M}_k(T)/\tilde{M}_k$ vs. the dimensionless temperature, $\Theta$. Of course, for $T = 0$, $\tilde{M}_k(0)/\tilde{M}_k = 1$. As the temperature increases, the effective kink mass decreases. The points represent the kink mass extracted from the numerical simulations, while the error bars were obtained by

propagating the standard deviation of the ensemble average. It is quite clear that the effective kink mass tracks the numerical values quite well. In fact, within the validity of our approximations, the "averaged" value for the effective kink mass is $0.75\tilde{M}_k$. Also, since the mass extracted from the simulations depends on the filter cutoff length $\Delta L$, the reasonable agreement between theory and numerical experiment offers indirect support for our choice of $\Delta L = 3$. For very small and very large temperatures the theory fails to track the numerical data. At large temperatures $\Theta \geq 0.25$, the one-loop approximation breaks down, while for low temperatures $\Theta \leq 0.12$, the large pair nucleation time-scale precludes a proper statistical analysis (not enough experiments). However, the conclusion is quite clear: by controlling the dependence on lattice spacing of the simulations we were able, within the validity of our approximations, to obtain the correct effective potential that should be used when comparing theory and numerical experiment.

---

[1] E. Kolb and M. Turner, *The Early Universe* (Addison-Wesley, New York, 1990).

[2] W. H. Zurek, Phys. Rep. **276**, 177–221 (1996); G. E. Volovik and T. Vachaspati, Int. J. Mod. Phys. **B10**, 471–521 (1996)[cond-mat/9510065].

[3] G. Parisi, *Statistical Field Theory* (Addison-Wesley, New York, 1988).

[4] M. Alford and M. Gleiser, Phys. Rev. **D48**, 2838–2844 (1993)[hep-ph/9304245].

[5] J. Borrill and M. Gleiser, Nucl. Phys. **B483**, 416–428 (1997) [hep-lat/9607026].

[6] P. Laguna and W. H. Zurek, Phys. Rev. Lett. **78**, 2519–2522 (1997); N. Antunes and L. Bettencourt, Phys. Rev. **D55**, 925 (1997).

[7] S. E. Trullinger and K. Sasaki, Physica **28** D, 181 (1987); D. Grecu and A. Visinescu, cond-mat/9304005.

[8] R. Rajaraman, *Solitons and Instantons* (North-Holland, Amsterdam, 1987).

[9] A. Heckler and M. Gleiser, Phys. Rev. Lett. **76**, 180–183 (1995)[hep-ph/9509347].

[10] F. J. Alexander and S. Habib, Phys. Rev. Lett. **71**, 955 (1993); F. J. Alexander, S. Habib, and A. Kovner, Phys. Rev. E **48**, 4282 (1993); S. Habib, cond-mat/9411058.

[11] A. I. Bochkarev and Ph. de Forcrand, Phys. Rev. Lett. **63** 2337 (1989); **64**, 2213 (1990); A. Krasnitz and R. Potting, Nucl. Phys. **B410**, 649 (1993).

[12] M. Alford, H. Feldman, and M. Gleiser, Phys. Rev. Lett. **68**, 1645–1648 (1992).

[13] P. Hänggi, F. Marchesoni, and P. Sodano, Phys. Rev. Lett. **60**, 256 (1988); see also M. Büttiker and T. Christen, Phys. Rev. Lett. **75**, 1895 (1995); Phys. Rev. Lett. **77**, 787 (1996).

[14] M. Büttiker and R. Landauer, Phys. Rev. **A23**, 1397 (1981).

[15] E. Weinberg and A. Wu, Phys. Rev. **D36**, 2474 (1987).
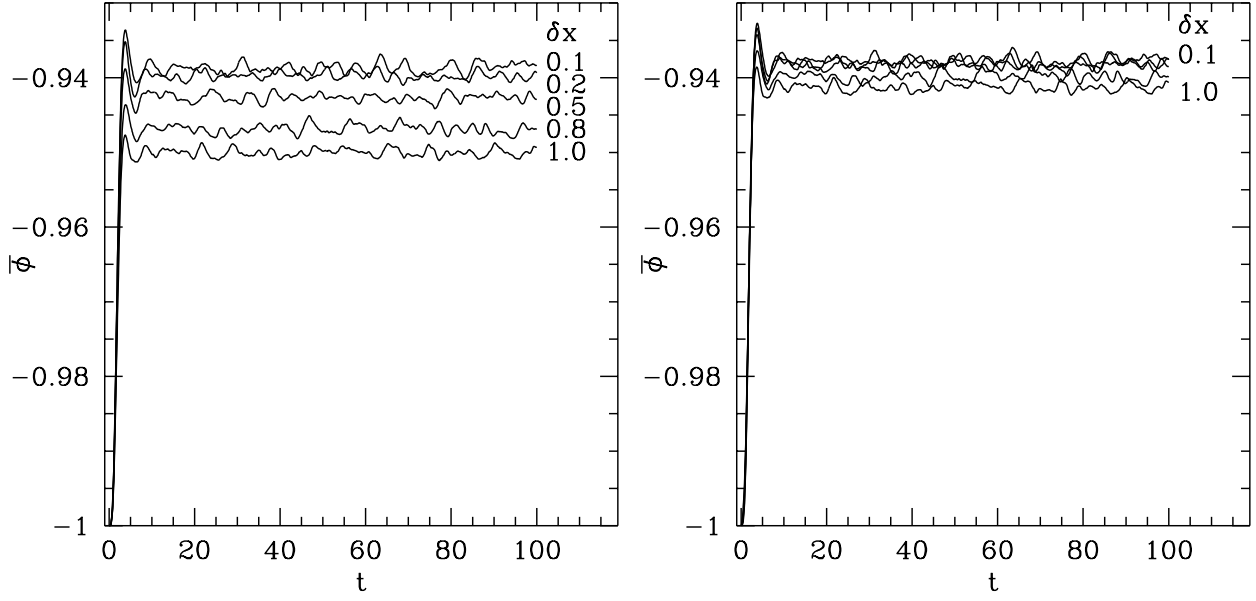
FIG. 1. Average field value $\bar{\phi}(t)$ for $T = 0.1$ using the tree-level potential, left, and the corrected potential, right.
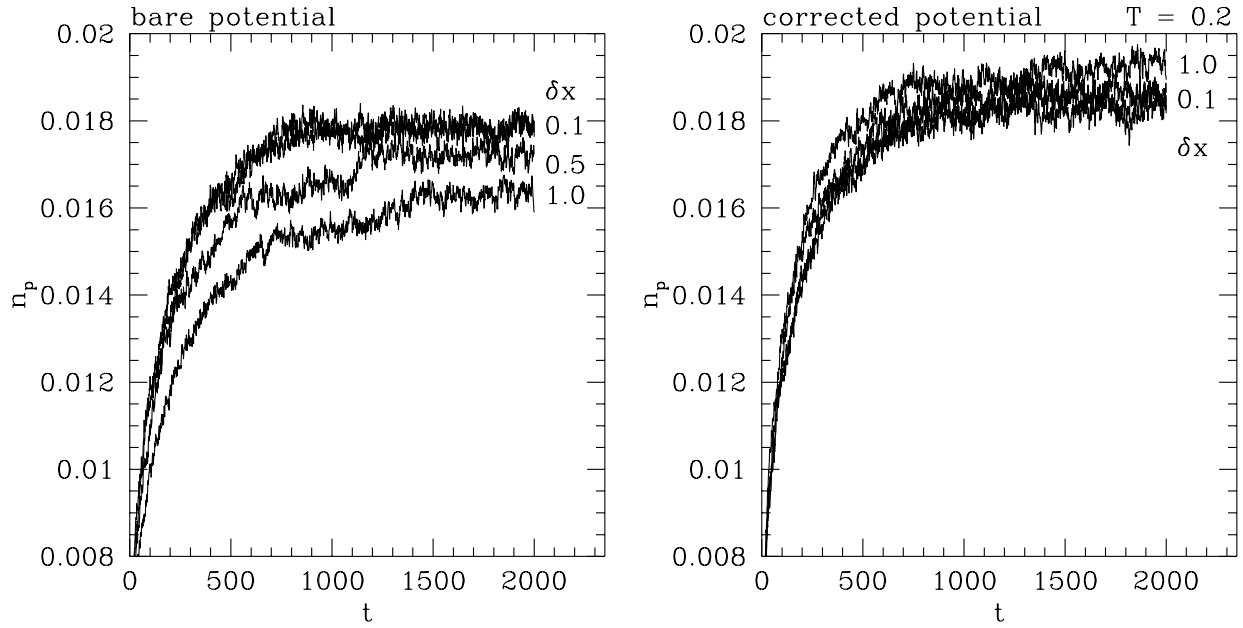


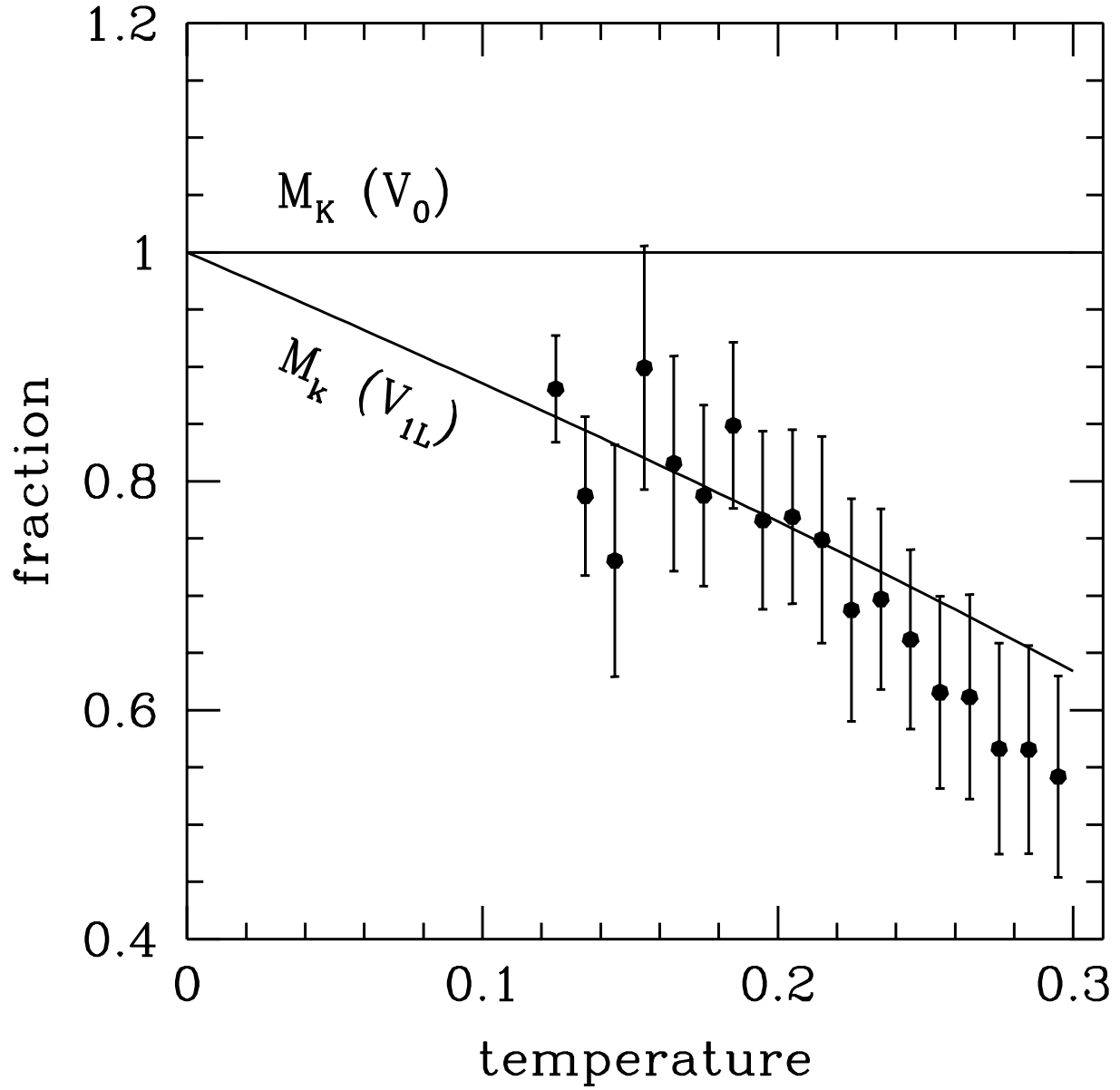FIG. 2. Density of kink-antikinks (half of density of zeros), for $T = 0.2$ and $\delta x = 1$, 0.5, 0.2, and 0.1.

FIG. 3. The ratio of the effective kink mass, $M_k(T)$, to the uncorrected kink mass, $M_k$, vs. the temperature.

| $\Delta L$ | $T = 0.15$ | $T = 0.20$ | $T = 0.25$ |
|---|---|---|---|
| 3 | $10.3 \pm 0.2$ | $39.0 \pm 0.5$ | $75.6 \pm 0.6$ |
| 5 | $8.9 \pm 0.2$ | $32.7 \pm 0.5$ | $62.0 \pm 0.5$ |
| 7 | $8.4 \pm 0.2$ | $29.8 \pm 0.4$ | $54.6 \pm 0.5$ |

Table 1: Number of kink-antikink pairs for different choices of the filter cutoff length $\Delta L$ and $T$.